Electron Paramagnetic Resonance and Magnetic Susceptibility Studies of Dimanganese Concanavalin A. Evidence for Antiferromagnetic Exchange Coupling†

Bradley C. Antanaitis,‡ Rodney D. Brown III,§ N. Dennis Chasteen,∥ Jonathan H. Freedman,⊥ Seymour H. Koenig,§ Henry R. Lilienthal,§ Jack Peisach,⊥ and C. Fred Brewer*,⊥

Department of Physics, Lafayette College, Easton, Pennsylvania 18042, Department of Molecular Pharmacology, Albert Einstein College of Medicine, Bronx, New York 10461, Department of Chemistry, University of New Hampshire, Durham, New Hampshire 03824, and IBM Thomas J. Watson Research Center, Yorktown Heights, New York 10598

Received April 22, 1987; Revised Manuscript Received June 30, 1987

ABSTRACT: The double Mn^{2+} complex of concanavalin A with bound saccharide (SMMPL) was examined by electron paramagnetic resonance (EPR) spectroscopy and magnetic susceptibility measurements. A room temperature X-band (9 GHz) EPR spectrum of SMMPL revealed a relatively weak, broad resonance in contrast to the spectrum with a six-line hyperfine-split pattern observed for the mononuclear, high-spin Mn^{2+} complex found in Ca^{2+}–Mn^{2+}–concanavalin A with saccharide present (SCMPL). The EPR spectrum of SMMPL at 77 K, however, consisted of a series of overlapping patterns of 11 hyperfine-split lines near $g = 2.0$ with members of each pattern separated by 47 G, half the value of the hyperfine splitting of SCMPL. These 11-line patterns are preserved at Q-band (35 GHz), indicating that the manganese ions in SMMPL form a spin-coupled, binuclear center. As expected for an exchange-coupled system, the EPR signal of SMMPL at 77 K saturates at a higher microwave power than those for SCMPL or Mn^{2+} aquoion. There is also a marked loss of EPR signal intensity for SMMPL between 4.2 and 1.4 K, which supports the view that the pair of manganese ions is exchanged-coupled. The temperature dependence of both the magnetic susceptibility and the low-temperature EPR spectral intensity can be explained by a model in which the two high-spin Mn^{2+} ions of SMMPL are antiferromagnetically exchanged-coupled with an isotropic coupling constant $J = 1.8$ cm^{-1} (for the spin Hamiltonian $\hat{H}_{ex} = J\vec{S}_1 \cdot \vec{S}_2$). Zero-field splitting D' was estimated to be 375 G from the EPR spectrum. The results provide direct evidence for coupled Mn^{2+} ions in the SMMPL complex, which is consistent with their binding at the S1 and S2 sites in the protein.

Concanavalin A (Con A)[1] is a metalloprotein, isolated from the jack bean (*Canavalia ensiformis*), and a member of the D-mannose/D-glucose binding lectins [cf. Goldstein and Hayes (1978)]. Its biological properties derive from its carbohydrate binding activity, which is regulated by the binding of metal ions. Early work established that the apoprotein is essentially devoid of carbohydrate binding activity and that addition of certain metal ions, typically Mn^{2+} and Ca^{2+}, completely restored activity (Kalb & Levitzki, 1968). Recently, the detailed mechanism of metal ion binding and activation of the protein has been elucidated [cf. Brewer et al. (1983a)].

Each monomeric unit of Con A can bind divalent metal ions at two sites: S1, the "transition metal" site, and S2, the "calcium" site, which is formed once S1 is occupied (Kalb & Levitzki, 1968). NMRD measurements of the interaction of Mn^{2+} and Ca^{2+} with apo-Con A showed that binding of Mn^{2+} to the S1 site and Ca^{2+} to the S2 site leads to the formation of a metastable complex in an inactive conformation, called "unlocked", which then converts to an active conformation, called "locked" (Brown et al., 1977; Koenig et al., (1978). These two conformations are largely distinguished by their affinities for metal ions and for saccharides. The locked conformation (PL) tightly binds both Mn^{2+} (M) and Ca^{2+} (C); when bound with metals, the protein (CMPL) possesses the full saccharide binding activity of the native lectin. The unlocked conformation weakly binds both metal ions and saccharide and is the predominant conformation of the apoprotein (Brown et al., 1977).

In the absence of Ca^{2+}, 2 molar equiv of Mn^{2+} bind to the apoprotein to form a locked ternary complex, MMPL, in a manner analogous to the formation of CMPL but with much slower kinetics (Brown et al., 1977). Studies by Harrington and Wilkins (1978) indicated that MMPL possesses full saccharide binding activity. Brewer et al. (1983b) showed that addition of α-MDM to a solution of Mn^{2+} and apo-Con A resulted in the rapid formation of a stable saccharide–MMPL complex (SMMPL), which bound Mn^{2+} tighter than MMPL due to the mass action effects of saccharide binding.

X-ray crystallographic studies of CMPL show that the metal ions in the S1 and S2 sites are 4.25 Å apart and bridged by two carboxyl ligands arising from aspartic acid residues 10 and 19 [cf. Hardman et al. (1982)]. If this structure is maintained in SMMPL, then one would expect the pair of bound Mn^{2+} ions, which are individually paramagnetic, to

† This work was supported in part by Grant CA-16054 and Core Grant P30 CA-13330 from the National Cancer Institute, Department of Health, Education, and Welfare (C.F.B.), by Grants AM 15056 (B.C.A.), GM 20194 (N.D.C.), and HL-13399 (J.P.) from the National Institutes of Health, and by a Summer Research Fellowship from Lafayette College (B.C.A.).

‡ Lafayette College.
§ IBM Thomas J. Watson Research Center.
∥ University of New Hampshire.
⊥ Albert Einstein College of Medicine.

[1] Abbreviations: Con A, concanavalin A with unspecified metal ion content and conformation state; CMPL, concanavalin A in the locked conformation (PL) with Ca^{2+} (C) at the S2 site and Mn^{2+} (M) at the S1 site; SMMPL, concanavalin A in the locked conformation with Mn^{2+} at the S1 and S2 sites and with bound saccharide (typically α-MDM); α-MDM, methyl α-D-mannopyranoside; EPR, electron paramagnetic resonance; NMRD, nuclear magnetic relaxation dispersion (the magnetic field dependence of the spin–lattice relaxation rate of solvent protons).

0006-2960/87/0426-7932$01.50/0

interact magnetically, e.g., by a spin–spin dipolar or an exchange-coupled mechanism (Griffith, 1972). The present studies provide direct evidence for the formation of such a binuclear Mn^{2+} protein complex.

Materials and Methods

Sample Preparation. Native Con A was obtained from Miles-Yeda (lot 172) from which apo-Con A was prepared according to the method of Brown et al. (1977). Manganese chloride tetrahydrate and calcium chloride dihydrate, as well as buffer salts, were obtained from Fisher Chemicals. Distilled, deionized water was used throughout. All samples were prepared in 0.1 M potassium acetate buffer, pH 6.4, containing 0.9 M potassium chloride. Protein concentrations, reported as monomeric units of 27 kDa, was determined spectrophotometrically at pH 5.6 in the same buffer by using the extinction coefficient at 280 nm of $A^{1\%,1cm} = 12.4$ (Yariv et al., 1968).

CMPL was typically prepared by adding 0.9 molar equiv of Mn^{2+} and 2 molar equiv of Ca^{2+} from 0.1 M stock solutions of each with a microliter syringe to a solution of apo-Con A and then dialyzing out the excess metal ions (Brown et al., 1977). SMMPL was typically formed by adding 1.8 molar equiv of Mn^{2+} and 0.1 M α-MDM to a solution of apo-Con A and then waiting for the complex to form by incubating the solution for approximately 5 days at room temperature (Brewer et al., 1983b). The CMPL and SMMPL complexes were characterized by NMRD analysis, as previously described (Brewer et al., 1983b), prior to EPR and magnetic susceptibility studies. Total Mn^{2+} in each sample was determined by NMRD analysis of an acidified aliquot and by atomic absorption spectrometry (Brewer et al., 1983b). Free Mn^{2+} in the sample solution was determined by NMRD measurements (Brewer et al., 1983b).

EPR Measurements. X-band (9 GHz) EPR spectra were recorded at 298 and 77 K with a Varian E-112 spectrometer equipped with a Varian E-231 multipurpose cavity. The frequency and magnetic field strength were monitored with a Systron-Donner frequency counter and a Varian NMR gaussmeter, respectively. An Apple II Plus microcomputer interfaced directly with the spectrometer was used to store and analyze spectral data.

Room temperature spectra of Mn^{2+} aquoion, CMPL, and MMPL were obtained with samples held in a quartz flat cell (60 × 10 × 0.25 mm). In addition, protein samples were prepared in the presence of α-MDM to give SCMPL and SMMPL, respectively. Identical samples were later frozen in quartz EPR tubes and examined at 77 K. The Mn^{2+} aquoion sample studied at 77 K was prepared from Mn^{2+}–acetate and diluted with ethylene glycol (50% v/v) in equal volumes to ensure glass formation upon freezing. Power saturation studies of manganese resonances from CMPL, SMMPL, and Mn^{2+} aquoion were carried out at 77 K. The microwave power was adjusted with the attenuation dial of the spectrometer.

EPR spectra taken between 1.4 and 4.2 K were recorded with a Varian E-9 spectrometer equipped with a Varian E-245 double Dewar apparatus. The temperature was varied as previously described (Antanaitis et al., 1980). Saturation of the EPR resonances was avoided by studying samples in a range where the EPR signal intensity was proportional to the square root of the microwave power. The temperature dependence of the EPR spectral intensity near $g = 2.0$ was determined from the double integral of the first-order derivative spectrum at nonsaturating power levels. Integrations were extended from 1000 G on either side of $g = 2.0$.

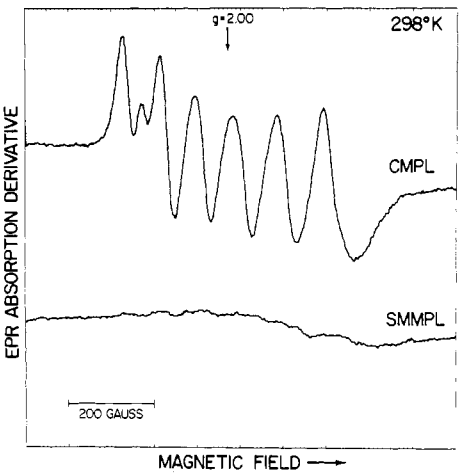

FIGURE 1: X-band EPR spectra of CMPL and SMMPL at 298 K. The SMMPL sample contained 0.38 mM apo-Con A, 0.57 mM Mn^{2+}, and 0.1M α-MDM in pH 6.4 buffer (0.1 M potassium acetate and 0.9 M potassium chloride). The CMPL sample contained 0.64 mM apo-Con A, 0.60 mM Mn^{2+}, and 2.0 mM Ca^{2+} in the same pH 6.4 buffer. EPR operating conditions: modulation amplitude 5 G, microwave power 20 mW, time constant 3 s, and scan rate 67 G/min.

Q-band (35 GHz) spectra were obtained at 120 ± 2 K with a Varian Q-band bridge and spectrometer console interfaced to a Harvey-Wells 12-in. magnet. The cavity was immersed in a stream of cold nitrogen gas and the temperature measured with a copper–Constantan thermocouple located inside the cavity. Spectra were recorded and stored with a Minc-23 computer (Digital Equipment Corp.). The magnetic field was calibrated with a Micro Now NMR gaussmeter. The g factors and hyperfine splittings were determined relative to Mn^{2+} doped in calcium oxide ($g = 2.001$; $a_0 = 86.28$ G).

Magnetic Susceptibility Measurements. Magnetic susceptibility measurements were made on an automated recording Faraday balance magnetometer, between 5 and 250 K (McGuire & Flanders, 1969). Samples contained in sealed quartz ampules were suspended from one arm of the self-adusting Ainsworth balance. The temperature was maintained by keeping the sample in a helium exchange gas atmosphere and measured using a thermocouple. The susceptibility was determined from the slope of the force on the sample, at a given temperature, as a function of field H.

The paramagnetic component of the protein susceptibility was calculated by subtracting the susceptibility of an apo-Con A sample containing saccharide from that of the Mn^{2+}–protein samples with saccharide at equal concentrations of protein.

Results

EPR Spectra of Mn^{2+}–Con A Complexes. The X-band EPR spectra of CMPL at 298 K shows the six-line hyperfine-split pattern near $g = 2.0$ characteristic of high-spin Mn^{2+} ion an "octahedral" environment (Figure 1). The splitting between successive lines is 95 G, and no additional features are evident. The spectrum of CMPL is similar to that of the Mn^{2+} aquoion, which also has 95-G hyperfine splittings. Addition of α-MDM has no effect on the EPR spectrum.

At 298 K SMMPL exhibits a low-intensity spectrum near $g = 2.0$ (Figure 1). The hyperfine-split pattern characteristic of mononuclear Mn^{2+} complexes is absent. At high spectrometer gains, resonances near g of 1.94 and 2.59 are detected, but hyperfine structure is not discernible. Dimanganese Con A prepared in the absence of saccharide has an EPR spectrum at room temperature virtually identical with that of Mn^{2+} aquoion, suggesting that this signal arises from the free Mn^{2+} known to be in equilibrium with MMPL (Brown et al., 1979).

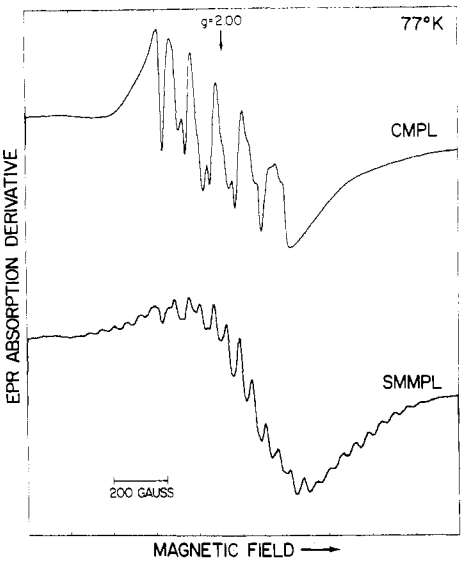

FIGURE 2: X-band EPR spectra of CMPL and SMMPL taken at 77 K with a 200-G spectral width. The concentrations of the samples were the same as in Figure 1. EPR instrumental conditions were the same as those described in Figure 1.

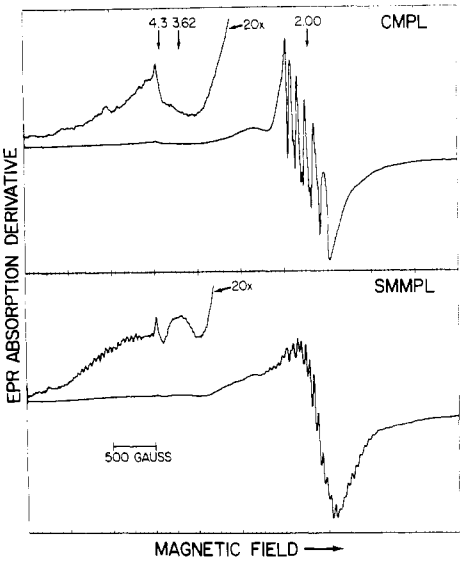

FIGURE 3: X-band EPR spectra of CMPL and SMMPL at 77 K, 500-G spectral width. The concentrations of the samples were the same as in Figure 1. EPR instrumental conditions were the same as those described in Figure 1.

The 77 K spectrum of CMPL resembles that of Mn^{2+} aquoion, having six hyperfine lines separated by 92.1 ± 0.9 G, each of which is further split into three components with separations of about 30 G due to second-order zero-field effects on the $M_z = \pm^1/_2$ states (Figure 2). In addition to the resonance near $g = 2$, additional resonances are observed near $g = 2.5$ and 4.3 (Figure 3). The weak $g = 4.3$ signal is attributed to rhombic high-spin ferric iron that is often found as a contaminant in protein samples (Tsibris & Woody, 1970).

In contrast, the spectrum of SMMPL at 77 K (Figure 2) is centered at $g = 1.927$ and consists of at least 32 resonance lines split by 47.1 ± 0.9 G, a splitting precisely half that of both CMPL and Mn^{2+} aquoion. Some of these lines also have a 3-fold splitting with components separated by 22 G, which is attributed to a small amount of mononuclear Mn^{2+}–Con A in the sample (less than 10%). Other resonances are observed near $g = 6.78$, 3.65, 2.86, 2.49, and 1.52 (Figure 3). The signal near $g = 6.78$ consists of approximately 20 hyperfine lines with splittings in the range of 47–49 G. Additional lines are present near $g = 4.27$, but these are partially obscured by the $g = 4.27$ rhombic iron resonance.

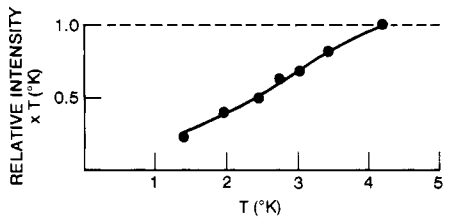

FIGURE 4: Temperature dependence of the $g = 2.0$ region of the X-band EPR signal of SMMPL from 1.4 to 4.2 K. The dashed line indicates the behavior expected for an isolated ground-state doublet. The solid line is a fit obtained with $J = 1.8$ cm^{-1} as described under Materials and Methods. The SMMPL sample contained 0.85 mM apo-Con A, 1.42 mM Mn^{2+}, and 0.1 M α-MDM in pH 6.4 buffer (0.1 M potassium acetate and 0.9 M potassium chloride).

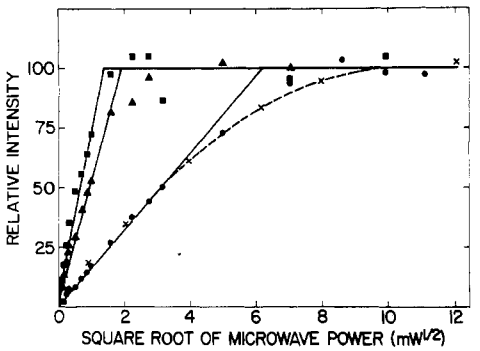

FIGURE 5: Power saturation curves for the Mn^{2+} aquoion (■), CMPL (▲), and SMMPL (●). The dashed line (-×-) represents a fit using the power saturation equation on p 259 of Rupp et al. (1978) with $b = 1$ and $P_{1/2} = 38$ mW. The solid line represents the behavior expected for a ground-state Kramers doublet. The concentrations of CMPL and SMMPL were the same as in Figure 1. The concentration of Mn^{2+} aquoion was 0.6 mM in pH 6.4 buffer (0.1 M potassium acetate and 0.9 M potassium chloride).

Of particular interest is the structure seen for SMMPL in the high-field portion of the $g = 1.927$ signal, near 3750 G (Figures 2 and 6A). Beginning at the high-field end of the spectrum and progressing to lower field, there is an 11-line progression with intensities approximately in the ratio of 1:2:3:4:5:6:5:4:3:2:1. There appears to be a similar pattern in the low-field portion of the spectrum, near 2950 G. Spectra obtained at fields between 1000 and 4200 G reveal similar overlapping bands of apparently 11 lines, each with hyperfine splittings close to 47 G.

At 4.2 K (not shown) the same hyperfine structure for SMMPL near $g = 2.0$ was detected as at 77 K. Resonances at low fields (i.e., below 2300 G) are either very weak or not detectable. As the temperature of the sample is lowered from 4.2 to 1.4 K, there is a substantial decrease in the spectral intensity, with this loss more apparent in the wings of the spectrum than in its central portion. The relative integrated intensities of the spectrum between 2440 and 4140 G multipled by the temperature and normalized to the intensity observed at 4.2 K are shown in Figure 4. Between 4.2 and 2.46 K the intensity decreases by almost 50%. An even greater decrease occurs between 2.46 and 1.4 K.

Saturation Characteristics of Mn^{2+} Complexes at 77 K. The level of microwave power required to half saturate SMMPL, CMPL, and Mn^{2+} aquoion was determined from plots of EPR signal intensity versus the square root of the microwave power (Figure 5). At nonsaturating power levels there is a linear relationship between the square root of the microwave power and the magnitude of the EPR absorption for all three samples, with a correlation coefficient of 0.98.

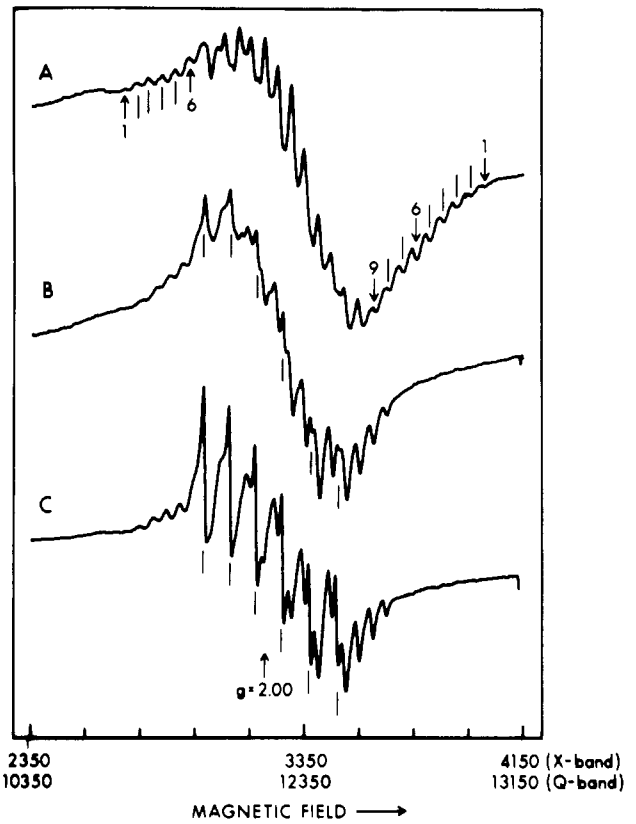

FIGURE 6: Comparison of X-band (A) and Q-band (B and C) EPR spectra of SMMPL at different microwave powers (T = 120 K). In (A) high-field arrows bracket 9 of the 11 lines of a Mn dimer hyperfine pattern. As expected for such patterns the splitting is only half that found for the corresponding monomer and the sixth (center) line is more intense than either of its neighbors. On the low-field side only six lines can be discerned. Positions of monomer lines are indicated by vertical lines in (B) and (C). EPR operating conditions: (A) modulation amplitude 5 G, microwave power 20 mW, time constant 3 s, scan rate 67 G/min, gain, 8×10^3; (B) modulation amplitude 2.5 G, microwave power 40 mW, time constant 0.03 s, scan rate 250 G/min, gain 40; (C) same as (B) except microwave power 0.3 mW, time constant 0.3 s, scan rate 125 G/min, and gain 2×10^2.

At higher power levels the signal intensity increases very little with concomitant increases in microwave power. The $P_{1/2}$ for CMPL is 4.0 mW, which is comparable to that of the Mn^{2+} aquoion (3.1 mW), while the value for SMMPL is 36.6 mW for essentially the same concentration of Mn^{2+}.

Q-Band EPR at 120 K. The Q-band spectrum of SMMPL at 120 K is similar to the X-band spectrum, having at least 25 lines with splittings of 47 G (Figure 6B). The Q-band spectrum, however, also shows six readily saturable lines with splittings close to 94 G near g = 2.0, attributable to either free Mn^{2+} aquoion or mononuclear Mn^{2+}–Con A (parts B and C of Figure 6). The hyperfine lines in the high-field portion of the spectrum appear to be absent in the Q-band spectrum (cf. parts A and B of Figure 6), although at higher gains some weak lines are observed. Also, at this high temperature and higher frequency no signals other than those near g = 2.0 are detected.

Magnetic Susceptibility of SCMPL and SMMPL. The magnetization of SCMPL at a field strength of 2.4 T increases as the temperature is lowered from 250 to 5 K (Figure 7), consistent with the expected behavior for noninteracting spins. Throughout the entire temperature range of the experiment, the data are well represented by the Brillouin function for a spin $^5/_2$ paramagnet having a g factor and Mn^{2+} concentration of 1.927 and 0.63 mM, respectively, as shown by the solid curve (Figure 7). The concentration of Mn^{2+} giving the best

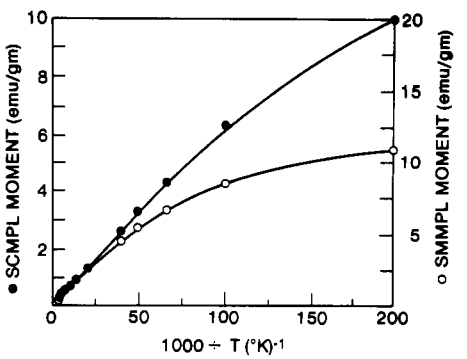

FIGURE 7: Magnetic susceptibility of SCMPL and SMMPL as a function of temperature. Solid lines represent fits obtained as discussed under Theory. The SCMPL sample contained 1 mM apo-Con A, 0.82 mM Mn^{2+}, 2 mM Ca^{2+}, and 0.1 M α-MDM in pH 6.4 buffer (0.1 M potassium acetate and 0.9 M potassium chloride). The SMMPL sample contained 1 mM apo-Con A, 1.62 mM Mn^{2+}, and 0.1 M α-MDM in the same buffer. A sample of 1 mM apo-Con A with 0.1 M α-MDM in the pH buffer was used as a control.

fit, though, is somewhat lower than that estimated from the known manganese content of the sample (0.81 mM).

On a per-manganese basis, the magnetization of SMMPL closely matches that of SCMPL between 250 and 40 K. Below 40 K, however, the magnetization of SMMPL begins to fall below that of the mononuclear complex, and at 5 K its value is only about half that found for SCMPL, indicative of Mn^{2+}–Mn^{2+} antiferromagnetic coupling.

THEORY

Determination of the Exchange-Coupling Constant. To account for the temperature dependence of both the EPR signal intensity and the magnetization measurements of SMMPL, identical spins of two high-spin Mn^{2+} ions were assumed to be coupled by an isotropic exchange Hamiltonian of the form: $\hat{H}_{ex} = J\hat{S}_1 \cdot \hat{S}_2$. With $S_1 = S_2 = {}^5/_2$, the net spin of the exchange-coupled system can assume the values 0, 1, 2, 3, 4, and 5. If the interaction is antiferromagnetic (i.e., J is positive), the S = 0 state lies lowest with excited multiplets obeying Lande's interval rule, with relative energies J, $3J$, $6J$, $10J$, and $15J$ above the ground-state singlet (Coles et al., 1960). The effective g factor of the spin-coupled system was taken as g = 1.927 and the isotropic hyperfine interactions as half that of the mononuclear complex, i.e., about 47 G (Slichter, 1955). The axial (D) and rhombic (E) zero-field splitting terms, which are known from single-crystal studies of CMPL (Meirovitch et al., 1974a) and the D value of SMMPL (vide supra) are much less than the electronic Zeeman term and were ignored in the present context.

The thermodynamic method of Peisach et al. (1971) was used to estimate J from the temperature dependence of the X-band EPR signal below 4.2 K. The value of J (1.8 ± 0.2 cm^{-1}) obtained by this approach also gives a satisfactory fit to the magnetization data (see below).

The magnetization associated with a particular multiplet of the spin-coupled manifold was described by a Brillouin function with the appropriate values of the resultant spin(s) allowed by the addition theorem of angular momentum (Slichter, 1965). The Brillouin function of each multiplet was then weighted by the Boltzmann and spin-multiplicity factors for the state (Carlin, 1966). Intensities of excited multiplets, all of which were assumed EPR-active, were calculated by using eq 1 of Okamura et al. (1965). These functions were then combined to yield the net magnetization as a function of temperature for the experimental field of 2.4 T. This model has three adjustable parameters: g, which was set equal to

1.927, the g value of the SMMPL complex; N, the concentration of the paramagnetic species, which was set equal to 0.81 mM (half the concentration of manganese in SMMPL); and J, the isotropic exchange-coupling constant, which was set equal to the J determined from the EPR data. The limits on J were estimated by considering the extreme values that still gave satisfactory fits to the data.

Discussion

The X-band EPR spectrum of CMPL with its six-line hyperfine splittings of 94 G is characteristic of magnetically dilute high-spin Mn^{2+} in an octahedral environment (Reed & Cohn, 1970; Meirovitch et al., 1974b). The complex EPR spectrum of SMMPL, however, suggests an interaction between a pair of specifically bound manganese ions. Isotropic exchange coupling of magnetically equivalent ions possessing nonzero nuclear spin (I) is suggested by a reduction in the effective hyperfine constant from A for the corresponding mononuclear complex to $A/2$ for the binuclear complex and an increase in the number of hyperfine lines from $2I + 1$ to $4I + 1$ (Griffith, 1972; Slichter, 1955). These resonances are weighted according to the possible ways of building up a given M_I (z component of nuclear spin) and span the same range in magnetic field as the hyperfine pattern of the mononuclear Mn^{2+} complex (Slichter, 1955).

For a pair of exchange-coupled manganese ions, with $I = {}^5/_2$, each fine structure resonance is expected to be split by an 11-fold pattern of hyperfine lines separated by 47 G with relative intensities in the ratio of 1:2:3:4:5:6:5:4:3:2:1. This pattern is found in the X-band EPR spectrum of SMMPL at 77 K, providing strong evidence for exchange coupling between the bound pair of manganese ions in SMMPL (Figure 2). The broad room temperature spectrum (Figure 1) is consistent with the exchange-coupling hypothesis, since, unlike Cu^{2+} dimers (Bertini et al., 1985, 1987), spin-coupled binuclear Mn^{2+} centers, with electron spin $S = {}^5/_2$, may be expected to exhibit shortened spin–lattice relaxation times due to coupling of the spin system to the lattice through the crystal field, electron exchange, and magnetic dipole contributions to the zero-field splitting terms. Shortened spin–lattice relaxation times also make it more difficult to saturate the signals arising from Mn^{2+} binuclear centers and thus account for the substantial increase in the microwave power required to half-saturate the EPR signal for SMMPL as compared to that of CMPL or Mn^{2+} aquoion (Figure 5).

The preservation of the pattern of lines with a separation of about 47 G in the Q-band spectrum of SMMPL (Figure 6) confirms the existence of a manganese dimer and indicates that the complexity of the X-band spectrum is not a result of overlapping resonances with different g values nor from second-order zero-field effects (Markham et al., 1981). The Q-band spectrum contains a small contribution from monomeric Mn^{2+} (most likely from SMPL), which accounts for some of the structural features of the X-band spectrum. The monomer lines are particularly sharp at 35 GHz, where line broadening from the second-order effect of D is largely absent. The level of monomeric Mn^{2+} contamination does not affect the interpretation of the magnetization data. Because the mononuclear Mn^{2+} signal is saturated at low temperature, it is unlikely that it influences the EPR spectral intensity measurements.

The loss of intensity in certain features of the Q-band spectrum suggests that part of the complexity of the X-band spectrum arises from transitions with forbidden character (Meirovitch et al., 1974a,b; Markham, 1981; Markham et al., 1979). Last, we note that the occurrence of hyperfine-split resonances at very low fields ($g = 6.78$) in the X-band spectrum most likely represents the hyperfine splitting of a zero-field band arising from an excited multiplet ($S \geq 3$) of the spin-coupled manifold. Multiplets characterized by lower values of S or those arising from a mononuclear contaminant would not be expected to be split so far from $g = 2.0$ (Meirovitch et al., 1974a,b).

The decrease in EPR signal intensity of SMMPL between 4.2 and 1.4 K further supports an exchange-coupling mechanism and allows an estimate of the strength of the exchange interaction. Fitting the temperature dependence of the spectral intensity as described under Theory yields a value for J of 1.8 ± 0.2 cm^{-1}. This can be compared with the J value of 0.0193 cm^{-1} for pairs of Mn^{2+} ions in host crystals of $La_2Zn_3(NO_3)_{12}{\cdot}24H_2O$ (Wilkins & Culvahouse, 1976). The loss of spectral intensity at low temperature arises from the decreased population of the magnetic states as the temperature is lowered, substantiating antiferromagnetic coupling.

The magnetic susceptibility data for SMMPL also support antiferromagnetic coupling. Using the value of J found by fitting the low-temperature EPR data to a Boltzman distribution, one can quantitatively account for the decrease of the magnetization for SMMPL as compared to SCMPL. Thus, both the low-temperature magnetization curve and the EPR spectral intensity data indicate that the pair of high-spin manganese ions of SMMPL is coupled antiferromagnetically.

The magnitude of the exchange coupling between the spins of a pair of manganese ions in SMMPL indicates that they are <10 Å apart. If the second Mn^{2+} ion occupies the S2 site normally occupied by Ca^{2+} [an assumption in accord with metal ion displacement studies as well as recent NMRD studies (Brown et al., 1977; Brewer et al., 1983b)], then the metal ions would be separated by approximately 4.25 Å, on the basis of X-ray crystallographic data for CMPL (Hardman et al., 1982). Such a configuration would also suggest that the spins are coupled at least in part by a super exchange mechanism involving the carboxylate groups of aspartic acid residues, although carboxylate groups are not known to be effective propagators of the exchange interaction (Ball, 1969; Murray, 1974). Direct overlap of metal d orbitals might also play a role in the exchange interaction, as suggested from recent calculations by Hopfield (1974) and Jortner (1976) showing that appreciable electron-exchange integrals can result from the direct overlap of rapidly decaying wave functions originating on sites separated by 10 Å or more. The presumed separation distance of the manganese ions of SMMPL falls well within that limit.

When the isotropic exchange term is dominant in the spin Hamiltonian and $E \ll D$, the 11-line "parallel" hyperfine patterns in the wings of the spectrum should be separated by $2D'$ ($D' = D/g\beta$). The separation between these progressions in the X-band spectrum gives a D' value of 375 G. A value of 400 G is estimated from the "perpendicular" features of the Q-band spectrum. Although the D' value contains a contribution from the magnetic dipole coupling between Mn^{2+} centers, the calculation of the metal–metal separation is not straightforward. This calculation would require a knowledge of the single ion zero-field tensors and their orientations relative to the dipole coupling tensor (Chao, 1973; Smith & Pilbrow, 1974). The contribution of the anisotropic exchange interaction to D' must be known or estimated as well. Such a calculation is beyond the scope of the present work.

Summary

The results of the present study confirm and extend our previous studies, which indicated that Mn^{2+} can bind to the

S1 and S2 sites of Con A to form a fully active complex that binds saccharide (SMMPL) (Brown et al., 1977; Brewer et al., 1983b). Magnetic susceptibility measurements indicate antiferromagnetic coupling between two Mn^{2+} ions in SMMPL, and EPR measurements have permitted estimation of the zero-field splitting in this system. The magnetic parameters obtained for SMMPL in the present study may be useful for comparing the results of similar disubstituted Mn^{2+} ion binding proteins, such as those found in chlorophyll dimers [cf. Brudvig and Crabtree (1986)].

ACKNOWLEDGMENTS

We thank Bert Olsen and Bernie Gilbert of the IBM Thomas J. Watson Research Center for the atomic absorption analyses of metal ion content.

REFERENCES

Antanaitis, B. C., Aisen, P., Lilienthal, H. R., Roberts, R. M., & Bazer, F. W. (1980) *J. Biol. Chem. 255*, 11204–11209.

Ball, P. W. (1969) *Coord. Chem. Rev. 4*, 361–383.

Bertini, I., Lanini, G., Luchinat, C., Manchini, M., & Spina, G. (1985) *J. Magn. Reson. 63*, 56–63.

Bertini, I., Banci, L., Brown, R. D., III, Koenig, S. H., & Luchinat, C. (1987) *Inorg. Chem.* (submitted for publication).

Brewer, C. F., Brown, R. D., III, & Koenig, S. H. (1983a) *J. Biomol. Struct. Dyn. 1*, 961–997.

Brewer, C. F., Brown, R. D., III, & Koenig, S. H. (1983b) *Biochemistry 22*, 3691–3702.

Brown, R. D., III, Brewer, C. F., & Koenig, S. H. (1977) *Biochemistry 16*, 3883–3896.

Brudvig, G. W., & Crabtree, R. H. (1986) *Proc. Natl. Acad. Sci. U.S.A. 83*, 4586–4588.

Carlin, R. L. (1966) *J. Chem. Educ. 43*, 521–525.

Chao, C. C. (1973) *J. Magn. Reson. 10*, 1–6.

Christie, D. J., Munske, G. R., & Magnuson, J. A. (1979) *Biochemistry 18*, 4638–4644.

Coles, B. A., Orton, J. W., & Owen, J. (1960) *Phys. Rev. Lett. 4*, 116–117.

Goldstein, I. J., & Hayes, C. E. (1978) *Adv. Carbohydr. Chem. Biochem. 35*, 127–340.

Griffith, J. S. (1972) *Struct. Bonding (Berlin) 10*, 87–126.

Hardman, K. D., Agarwal, R. C., & Freiser, M. J. (1982) *J. Mol. Biol. 157*, 69–86.

Harrington, P. C., Moreno, R., & Wilkins, R. G. (1978) *Biochemistry 17*, 4245–4250.

Hopfield, J. J. (1974) *Proc. Natl. Acad. Sci. U.S.A. 71*, 3640–3644.

Jortner, J. (1976) *J. Chem. Phys. 64*, 4860–4867.

Kalb, A. J., & Levitzki, A. (1968) *Biochem. J. 109*, 669–672.

Kittel, C. (1968) *Introduction to Solid State Physics*, pp 427–451, Wiley, New York.

Koenig, S. H., Brewer, C. F., & Brown, R. D., III (1978) *Biochemistry 17*, 4251–4260.

Markham, G. D. (1981) *J. Biol. Chem. 256*, 1903–1909.

Markham, G. D., Rao Nageswara, B. D., & Reed, G. H. (1979) *J. Magn. Reson. 33*, 595–602.

Meirovitch, E., Luz, Z., & Kalb, J. A. (1974a) *J. Am. Chem. Soc. 96*, 7538–7542.

Meirovitch, E., Luz, Z., & Kalb, A. J. (1974b) *J. Am. Chem. Soc. 96*, 7542–7546.

Murray, K. S. (1974) *Coord. Chem. Rev. 12*, 1–35.

Okamura, M. Y., & Hoffman, B. M. (1969) *J. Chem. Phys. 51*, 3128–3129.

Peisach, J., Blumberg, W. E., Lode, E. T., & Coon, M. J. (1971) *J. Biol. Chem. 246*, 5877–5881.

Reed, G. H., & Cohn, M. (1970) *J. Biol. Chem. 245*, 662–664.

Rupp, H., Rao, K. K., Hall, D. O., & Cammack, R. (1978) *Biochim. Biophys. Acta 537*, 255–269.

Slichter, C. P. (1955) *Phys. Rev. 99*, 479–480.

Smart, J. S. (1966) *Effective Field Theories of Magnetism*, W. B. Saunders, Philadelphia.

Smith, T. D., & Pilbrow, J. R. (1974) *Coord. Chem. Rev. 13*, 173–278.

Tsibris, J. C. M., & Woody, R. W. (1970) *Coord. Chem. Rev. 5*, 417–458.

Wilkins, R. W., & Culvahouse, J. W. (1976) *Phys. Rev. B: Solid State 14*, 1830–1841.

Yariv, J., Kalb, A. J., & Levitzki, A. (1968) *Biochim. Biophys. Acta 165*, 303–305.